BIOCHEMISTRY
including biophysical chemistry & molecular biology
Article

Biochemistry **2009,** *48,* 10473–10482 10473
DOI: 10.1021/bi901238t

Monomer−Dimer Equilibrium in Glutathione Transferases: A Critical Re-Examination

Raffaele Fabrini,[‡,@] Anastasia De Luca,[§,@] Lorenzo Stella,[‡,@] Giampiero Mei,[∥] Barbara Orioni,[‡] Sarah Ciccone,[§] Giorgio Federici,[⊥] Mario Lo Bello,[§] and Giorgio Ricci*[,‡]

[‡]*Department of Chemical Sciences and Technologies, University of Rome "Tor Vergata", 00133 Rome, Italy,* [§]*Department of Biology, University of Rome "Tor Vergata", 00133 Rome, Italy,* [∥]*Department of Experimental Medicine and Biochemical Sciences, Univerity of Rome "Tor Vergata", 00133 Rome, Italy, and* [⊥]*Children's Hospital IRCCS "Bambin Gesù", 00165 Rome, Italy.* [@]*These authors equally contributed to this work.*

Received July 20, 2009; Revised Manuscript Received October 1, 2009

ABSTRACT: Glutathione transferases (GSTs) are dimeric enzymes involved in cell detoxification versus many endogenous toxic compounds and xenobiotics. In addition, single monomers of GSTs appear to be involved in particular protein−protein interactions as in the case of the pi class GST that regulates the apoptotic process by means of a GST−c-Jun N-terminal kinase complex. Thus, the dimer−monomer transition of GSTs may have important physiological relevance, but many studies reached contrasting conclusions both about the modality and extension of this event and about the catalytic competence of a single subunit. This paper re-examines the monomer−dimer question in light of novel experiments and old observations. Recent papers claimed the existence of a predominant monomeric and active species among pi, alpha, and mu class GSTs at 20−40 nM dilution levels, reporting dissociation constants (K_d) for dimeric GST of 5.1, 0.34, and 0.16 μM, respectively. However, we demonstrate here that only traces of monomers could be found at these concentrations since all these enzymes display K_d values of $\ll$1 nM, values thousands of times lower than those reported previously. Time-resolved and steady-state fluorescence anisotropy experiments, two-photon fluorescence correlation spectroscopy, kinetic studies, and docking simulations have been used to reach such conclusions. Our results also indicate that there is no clear evidence of the existence of a fully active monomer. Conversely, many data strongly support the idea that the monomeric form is scarcely active or fully inactive.

Glutathione transferases (GSTs)[1] make up a superfamily of multifunctional enzymes involved in cell detoxification and excretion of endogenous or exogenous toxic compounds (*1*). One prominent role of GSTs is represented by the conjugation of the thiol group of GSH to the electrophilic center of organic compounds, but they also function nonenzymatically by binding nonsubstrate ligands and reactive compounds, leading to enhanced elimination of these molecules (*2*, *3*). In the past several decades, other protective functions of these enzymes have been discovered. For example, GSTP1-1 is involved in the regulation of the proapoptotic enzyme c-Jun N-terminal kinase (JNK) by means of a protein−protein interaction (*4*), and GSTM1-1 inhibits the apoptosis signal-regulating kinase (ASK1) by binding to ASK1 within the C-terminal portion of GSTM1 (*5*). Therefore, GSTs are deeply involved in apoptosis regulation (*6*, *7*). Another role of these enzymes only recently discovered is the protection of the cell against the excess of nitric oxide (*8*). This multiplicity of beneficial functions possibly explains why GSTs are widely expressed in almost all organisms from plants and bacteria to humans. From a structural point of view, mammalian cytosolic GSTs are dimeric proteins that have been grouped into eight classes (alpha, kappa, mu, omega, pi, sigma, theta, and zeta), on the basis of amino acid sequence, immunological properties, and substrate specificity (*9*−*15*). Today, the crystal structure of at least one representative member of each class has been determined, showing that all cytosolic GSTs display very similar tertiary architectures. In particular, the subunit interface shows a hydrophobic region represented by a well-studied "lock and key" interaction and a hydrophilic region in which a number of electrostatic interactions between charged residues are present. In the past, many attempts have been made to find experimental conditions that promote the dissociation into single subunits and to study the catalytic and structural properties of the isolated monomers. In fact, the monomer−dimer transition of GSTs has important physiological and pharmacological impacts and does not have merely theoretical interest. For example, GSTP1-1 regulates the activity of JNK by means of a JNK−GST complex, where GSTP1-1 appears to be bound in a monomeric form (*4*). Unfortunately, previous studies concerning the monomer−dimer equilibrium and the possible catalytic competence of the GST monomers have reached conflicting conclusions. Many studies support the conclusion that GST monomers are inactive. For example, Aceto et al. found that at low detergent concentrations, GSTP1-1 dissociates into folded subunits, but in this monomeric form, the enzyme is completely inactive (*16*). A similar folded but inactive monomeric structure of GSTP1-1 was found by Abdalla et al. (*17*), who studied the dissociation of this enzyme after mutation of critical amino acids at the dimer interface. GSTP1-1 is secreted as a monomer into human plasma by platelets and

*To whom correspondence should be addressed: Department of Chemical Sciences and Technologies, University of Rome "Tor Vergata", via della Ricerca Scientifica, 00133 Rome, Italy. Phone: +390672594379. Fax: +3972594328. E-mail: riccig@uniroma2.it.

[1]Abbreviations: GST, glutathione *S*-transferase; JNK, c-Jun N-terminal kinase; CDNB, 1-chloro-2,4-dinitrobenzene; GSNO, *S*-nitrosoglutathione; DNDGIC, dinitrosyl-diglutathionyl-iron complex; DTNB, 2,2′-dithionitrobenzoic acid; TPE-FCS, two-photon excitation fluorescence correlation spectroscopy; K_d, dissociation constant of dimeric glutathione transferases.

Published on Web 10/01/2009

tumor cells, but the monomeric form is completely inactive (*18*). As a consequence of a single-point mutation in GSTA1-1, Sayed et al. (*19*) have also demonstrated that dimer dissociation and unfolding processes are closely coupled. For the mu class GST, it has been proven that the dimeric structure is required to maintain functional conformations at the active site on each subunit (*20*). That study also gave a first indication of a nanomolar value for the dissociation constant (K_d) for the native enzyme (12 nM). Again for the mu class GST, a double mutation at the subunit interface results in a stable, folded monomer that is almost fully inactive (*21*). These reports, all consistent with the conclusion that the monomers of GSTs are fully or severely impaired in their catalytic competence, have been contradicted by recent studies (*22*−*24*). On the basis of light scattering and sedimentation equilibrium data, the existence of relevant amounts of monomers of pi, alpha, and mu GSTs when these enzymes are present at nanomolar levels has been proposed. In fact, the dissociation constants calculated for these homodimeric proteins (5.1 μM for GSTP1-1, 0.34 μM for GSTA1-1, and 0.16 μM for GSTM2-2) predicted that, at the concentration used for the spectrophotometric activity assay (20−40 nM, 0.5−1 μg/mL), these enzymes would exist mainly as monomers (98% for GSTP1-1, 94% for GSTA1-1, and 90% for GSTM2-2), and consequently, their single subunits would be highly active. Site-directed mutagenesis and high KBr concentrations have also been used by the same group to force the monomerization process (*22*−*24*). Even in that case, sedimentation equilibrium and light scattering data were interpreted as suggesting that the monomeric form of GSTP1-1 and GSTM2-2 may be catalitically competent (*22*, *24*). This paper re-examines the question on the basis of different experimental approaches like static and dynamic fluorescence anisotropy and two-photon fluorescence correlation spectroscopy. Furthermore, to extend our investigation, we took into account two important properties of these enzymes, i.e., the cooperativity found in pi, alpha, and mu class GSTs for the binding of the substrate or specific inhibitors and the peculiar stabilization of GSH in the active site of each subunit due to a conserved Asp residue of the adjacent subunit. In fact, the monomerization of GSTs must be signaled by the disappearance of any cooperative phenomenon and also by a decreased affinity for GSH. Using these uncommon probes together with traditional approaches, we were able to check the oligomeric state of GSTs at very high dilutions, i.e., down to subnanomolar concentrations. Overall, both kinetic and fluorescence data indicate that the K_d values for all GST isoenzymes must be confined at or below the nanomolar range, values 1000 times lower than those reported in previous studies. These findings have also a deep impact on statements about the existence of active monomeric forms of GSTs.

EXPERIMENTAL PROCEDURES

Materials. GSH and 1-chloro-2,4-dinitrobenzene (CDNB) were obtained from Sigma-Aldrich. The fluorophore HiLyte Fluor 488 was purchased from AnaSpec Inc. (San Jose, CA). Dinitrosyl-diglutathionyl-iron complex (DNDGIC) was prepared as descibed previously (*25*). 2,2′-Dithionitrobenzoic acid (DTNB) was a Sigma product.

Expression and Purification of Native GSTP1-1, GSTA1-1, and GSTM2-2. Human GSTP1-1, GSTA1-1, and GSTM2-2 were expressed in *Escherichia coli* and purified as described previously (*25*−*27*). Enzyme concentrations are always expressed as moles of subunit per liter.

Labeling of GSTP1-1 with HiLyte Fluor 488. GSTP1-1 (88 μM) was incubated at 25 °C with 100 μM HiLyte Fluor 488 in the presence of 10 mM phosphate buffer saline (pH 7.0). After incubation for 30 min, the protein labeled with the fluorescent probe was passed through a gel filtration chromatography column (Sephadex G25, Amersham) to remove the excess of reagent. The fractions containing the labeled protein were pooled and analyzed for their protein content by absorbance at 280 nm. The contribution of HiLyte Fluor 488 to the absorption at 280 nm was estimated by the absorption value at 507 nm multiplied by 0.2 and subtracted from the total absorbance before calculation of protein concentration, using an extinction coefficient of 25460 M^{-1} cm^{-1} for the GST monomer (*28*). Titration of free protein thiol groups with DTNB (*29*) indicated that only one SH group for the monomer has reacted with the fluorescent probe.

Time-Resolved Fluorescence Anisotropy. Time-resolved fluorescence anisotropy experiments (20 °C) were performed on a Lifespec-ps setup (Edinburgh Instruments) equipped with automatic Glan-Thompson polarizers, a cooled microchannel plate detector, and a 440 nm pulsed diode laser (0.1 ps pulse width). Emission was collected at 480 nm (bandpass of 16 nm), through a 455 nm cutoff filter.

Steady-State Fluorescence Anisotropy. Fluorescence anisotropy experiments were performed on a Fluoromax 2 fluorimeter (Horiba Jobin Yvon), equipped with automatic Glan-Thompson polarizers (20 °C). Intrinsic fluorescence was measured with the following parameters: λ_{ex} at 280 nm (bandwidth of 7 nm), λ_{em} at 340 nm (bandwidth of 20 nm), and a 305 nm cutoff filter. The HiLyte Fluor 488 fluorescence was measured with λ_{ex} at 485 nm (bandwidth of 8 nm), λ_{em} at 526 nm (bandwidth of 10 nm), and a 495 nm cutoff filter. Each anisotropy value is the result of nine replicate measurements, with a 4 s averaging time for each polarizer orientation. Background counts were subtracted before anisotropy calculations.

Fluorescence Correlation Spectroscopy. Two-photon excitation fluorescence correlation spectroscopy (TPE-FCS) experiments were performed at 20 °C on an Alba FCS setup, equipped with a Chamaleon Ultra Ti-Sapphire laser (λ_{ex} = 880 nm) and a Nikon inverted microscope. Autocorrelation curves were measured for a 40 nM solution of GSTP1-1 labeled with HiLyte Fluor 488, and for the same solution after addition of 10 μM unlabeled protein. To prevent adsorption of protein to cell walls, cuvettes were pretreated with a 1 mg/mL bovine serum albumin solution and thoroughly washed.

Data fitting was performed with Vista-FCS (ISS, Inc., Champaign, IL), after calibration of the excitation volume with a 8 nM rhodamine 6G solution. All data result from the average of three independent experiments.

Standard Assay for GST Activity. GST activity was assayed in 0.1 M potassium phosphate buffer (pH 6.5) in the presence of 1 mM GSH and 1 mM CDNB (25 °C). The reaction was followed spectrophotometrically (double-beam Uvikon 940 Kontron spectrophotometer equipped with a cuvette holder) at 25 °C at 340 nm where the GSH−2,4-dinitrobenzene adduct absorbs (ε = 9600 M^{-1} cm^{-1}).

Kinetic Analysis. K_m^{GSH} values were calculated via variation of the GSH concentration from 0.1 to 1 mM by keeping constant the CDNB concentration at 1 mM at two different enzymatic concentrations for each isoform (1.0 and 0.04 μg/mL for GSTP1-1 and GSTA1-1 and 0.2 and 0.008 μg/mL for GSTM2-2). Kinetic

data were analyzed with GraphPad version 4.0. The data obtained by varying GSH concentrations were analyzed by being fit to the Hill equation. The dependence of K_m^{GSH} on CDNB concentration was studied at a fixed GSH concentration of 1 mM and a CDNB concentration varying from 0.25 to 1 mM. Data were analyzed plotting K_m^{GSH} values versus CDNB concentration to extrapolate K_m^{GSH} at 0 mM CDNB. The reported kinetic parameters represent the means of at least three different experimental sets.

Fluorescence Quenching. Dissociation constants for the GST−GSH complex were determined on the basis of the intrinsic fluorescence perturbation due to GSH binding. Experiments were performed at 25 °C using a single-photon counting spectrofluorometer (Fluoromax 2, Horiba Jobin Yvon). Excitation was at 295 nm, and emission was at 350 nm. In a typical experiment, the fluorescence intensity was measured before and after the addition of suitable amounts of GSH (from 0.01 to 4 mM) to a final concentration of 100 μg/mL (~4 μM) GSTs in 0.1 M potassium phosphate buffer (pH 6.5). Experimental data were corrected both for dilution and for inner filter effects and fitted to eq 1.

$$F_L = F_0 + (F_{max} - F_0)/(1 + K_d/[GSH]) \quad (1)$$

where F_0 is the protein fluorescence in the absence of GSH, F_L is the protein fluorescence in the presence of a given amount of GSH, and F_{max} is the protein fluorescence at saturating GSH concentrations.

DNDGIC Binding. Binding of DNDGIC to GSTP1-1 and GSTM2-2 was studied by incubating variable amounts of DNDGIC (from 0.2 nM to 0.4 μM) with fixed enzyme concentrations (0.8 nM for GSTP1-1 and 0.32 nM for GSTM2-2) in 0.1 M potassium phosphate buffer (pH 6.5). After preincubation for 30 s, 1 mM GSH and 1 mM CDNB were added and the enzymatic activity was followed spectrophotometrically at 340 nm (25 °C). Data were fitted to a biexponential decay equation.

Docking Simulations. Docking simulations were performed with AutodockTools 1.4.6 (*30*) using the hGST crystal structures in complex with glutathione [Protein Data Bank (PDB) entries 6GSS for GSTP1-1, 1PKW for GSTA1-1, and 1XW5 for GSTM2-2]. Polar hydrogen atoms were added geometrically, and Kollman united-atom charges were assigned (*31*). Docking experiments with GSH were performed using a nonflexible ligand. GSH charges were added manually by the Gasteiger−Marsili method (*32*) and by fixing the sulfhydryl of GSH as a deprotonated group. Grids of molecular interactions were calculated in a cubic box, with a size of 40 Å and a grid spacing of 0.375 Å, centered on the G-site. Docking was performed 100 times using the Lamarckian genetic algorithm, with the ligand initially in its crystallographic position and conformation, a population size of 150, and a maximum of 150000 energy evaluations and 27000 generations. Docking was performed with standard parameters (*32*) except step size parameters such as translation (angstroms per step), quaternion (degrees per step), and torsion (degrees per step) all set to 1.0. The 100 final docked conformations were ranked according to their binding free energy and clustered using a tolerance of 3 Å root-mean-square deviation (rmsd). Two different simulations were performed: (a) GSH docking to dimeric hGSTs (D) and (b) GSH docking to dimeric hGSTs after neutralization of the Asp residue participating in the G-site of the adjacent subunit (Asp 98 for GSTP1-1, Asp 101 for GSTA1-1, and Asp 105 for GSTM2-2) (D*). MOLMOL (*33*) was used for graphical interpretation and representation of results.

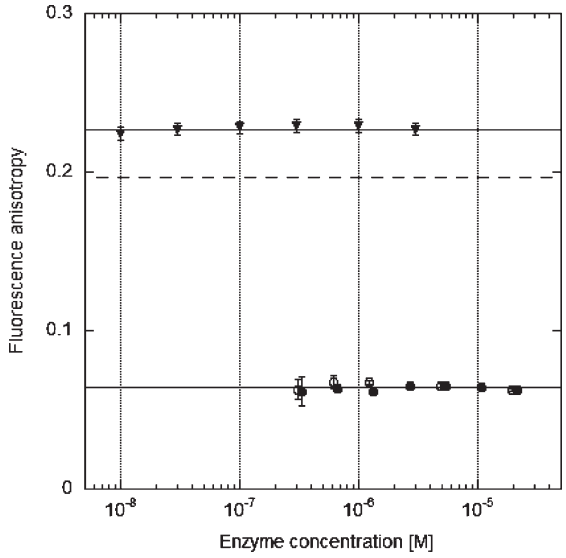

FIGURE 1: Steady-state anisotropy of the intrinsic Trp fluorescence of GSTP1-1 (●) and GSTA1-1 (○) and of the HiLyte Fluor 488 emission of labeled GSTP1-1 (▼). The horizontal dashed line represents the anisotropy value expected for monomeric HiLyte Fluor 488-labeled GST (0.197), based on the time-resolved measurements reported in Figure 2.

RESULTS

Fluorescence Experiments. According to the studies supporting a relatively easy dissociation of GSTs, GSTP1-1 displays a stronger propensity to monomerize (K_d = 5.1 μM) (*22*) when compared to the alpha (K_d = 0.34 μM) (*23*) and mu GSTs (K_d = 0.16 μM) (*24*). For this reason, we started our fluorescence experiments using this specific isoenzyme. Fluorescence anisotropy provides a direct determination of the rotational diffusion of a macromolecule, and thus of its molecular weight. In time-resolved fluorescence anisotropy experiments, the sample is excited with a pulse of linearly polarized light and the decay of the anisotropy of the emitted radiation polarization is measured over time. This allows the determination of the rotational correlation time of the macromolecule, which is proportional to its molecular weight (*34*). On the other hand, in steady-state anisotropy experiments, the sample is continuously illuminated by a stationary intensity of polarized light, and the measured anisotropy values correspond to an average of the anisotropy decay over the time window determined by the excited-state lifetime of the fluorophore being employed. As such, any change in the diffusional motions of the protein is reflected in a significant change in the value of the steady-state anisotropy, as found in our previous studies concerning the dimer-to-tetramer transition of the *Plasmodium falciparum* GST (*35*) and the monomer-to-dimer transition of superoxide dismutase (*36*). Figure 1 reports the steady-state fluorescence anisotropy of GSTP1-1 as a function of enzyme concentration. Intrinsic Trp fluorescence allowed the determination of anisotropy from 20 μM (where this protein would be mainly dimeric, according to the reported K_d value of 5.1 μM) to a protein concentration of ~0.3 μM (where it should be almost completely monomeric). However, no appreciable change was detected in the steady-state anisotropy. The same behavior was found for GSTA1-1 (Figure 1). To extend the concentration range to higher dilutions,

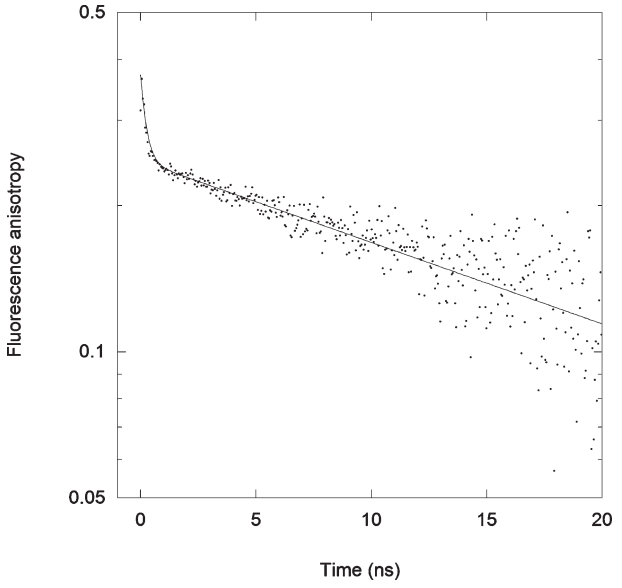

FIGURE 2: Time-resolved anisotropy of HiLyte Fluor 488 fluorescence of labeled GSTP1-1. The solid curve represents the best double-exponential fit. The protein concentration was 3 μM.

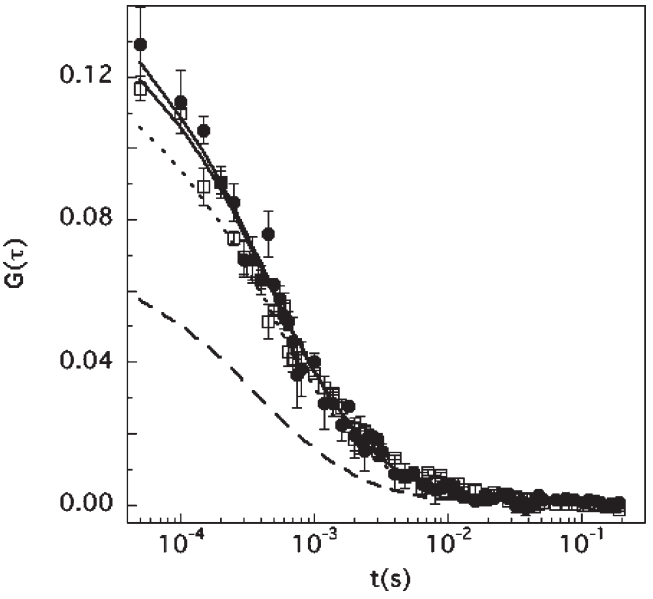

FIGURE 3: Fluorescence correlation spectroscopy autocorrelation data for 40 nM HiLyte Fluor 488-labeled GSTP1-1 before (●) and after (□) addition of 10 μM unlabeled GSTP1-1. Standard deviations were calculated by averaging three repeated measurements. The solid lines represent the best fits to the data. The dashed line is the autocorrelation curve expected in the case of complete dissociation of the GST dimers, assuming a diffusion coefficient of 85 $\mu m^2/s$ for the monomer (*39*). The dotted line is the autocorrelation curve expected for a 30% monomerization.

we employed the extrinsic fluorescence of a HiLyte Fluor 488 label, attached to one of the GSTP1-1 Cys residues. In this case, we were able to reach a protein concentration of 10 nM, with no appreciable variations in the steady-state anisotropy (Figure 1). These experiments prove an identical aggregation state for GSTP1-1 within the concentration range of 10^{-5} to 10^{-8} M. However, they do not provide any indication about the molecular mass of the protein that could be present as a dimer, or also as a monomer or in a higher oligomeric aggregation state, at all concentrations investigated.

To confirm the dimeric nature of the P1-1 enzyme under the conditions investigated, we measured the anisotropy decay of the HiLyte Fluor 488-labeled P1-1 enzyme (Figure 2). The decay could be satisfactorily fitted with a double-exponential decay with rotational times of 0.25 ns (associated fraction of 0.34) and 26 ns (associated fraction of 0.66), with a zero-time anisotropy of 0.37. The fast rotational time represents the segmental motions of the fluorophore, while the slow time is associated with the rotational diffusion of the protein; it corresponds to the rotational correlation time expected for the molecular mass of the dimer (*37*). From both static and dynamic fluorescence data, we can conclude that the extent of monomerization of GSTP1-1 at 10 nM is negligible. To estimate an upper limit for the dissociation constant, we calculated the expected steady-state anisotropy values for a completely dimeric or completely monomeric HiLyte Fluor 488-labeled enzyme, based on the time-resolved measurements (*34*). The expected steady-state anisotropy value for the dimer (r_d) is 0.225, in good agreement with the measured values, while for the monomer, the expected value (r_m) is 0.197 (dashed line in Figure 1), assuming a rotational correlation time of 13 ns. The minimum anisotropy value consistent with the observed data and experimental errors (r_{min}) is 0.220, which corresponds to the lower limit of the error bar at a protein concentration of 10 nM. This value would place an upper limit on the monomeric fraction of $(r_{min} - r_d)/(r_m - r_d)$ of 0.18, which corresponds to K_d values of < 0.8 nM.

A further confirmation of a very scarce or null monomerization, down to nanomolar concentrations, was provided by two-photon excitation fluorescence correlation spectroscopy experiments (Figure 3). The principle of FCS lies in the quantification of the magnitude and duration of fluorescence fluctuations caused by molecules freely diffusing in and out of the measurement volume. The magnitude of the fluctuations is related to the number of particles in the measurement volume, and the duration of fluctuations (as calculated by the autocorrelation function of the measured signal) to the characteristic time the particles take to cross the volume (i.e., to their hydrodynamic radius) (*38*). We performed FCS measurements for a 40 nM solution of labeled GSTP1-1 and for the same solution after the addition of 10 μM unlabeled enzyme. As shown in Figure 3, the two curves are quite similar, showing that no significant change in the protein association state occurred in this concentration range. This conclusion was confirmed by data fitting (see Experimental Procedures), which yielded a diffusion coefficient of 66 ± 8 $\mu m^2/s$ for the labeled protein and of 62 ± 4 $\mu m^2/s$ after the addition of unlabeled GST. According to Young et al. (*39*), the expected diffusion coefficient for the GSTP1-1 dimer is 68 $\mu m^2/s$ and 85 $\mu m^2/s$ for the monomer. Simulations (dotted line in Figure 3) indicate that a 30% monomerization would give a significant variation of the autocorrelation curve. Therefore, in our experiments, the monomerization is definitely $< 30\%$, which results in a K_d of < 10 nM.

Temperature-Dependent Cooperativity Used as a Probe of the Dimeric State of GSTP1-1. A few years ago, a peculiar temperature-dependent cooperative behavior of GSH binding was discovered for GSTP1-1 (*40*). This property, validated independently by using NMR analysis (*41*), probably helps to minimize changes in affinity toward GSH caused by low or high temperatures in vivo. In fact, this specific isoenzyme is strongly expressed in human skin, a tissue often exposed to thermal stress. The presence or absence of this particular mechanism may be a useful probe for checking the aggregation state of GSTP1-1 at low concentrations. In fact, an oligomeric structure is the *conditio*

sine qua non for the existence of a binding cooperativity in a protein that displays a single binding site per subunit. Given that cooperativity has been observed at 3 μM, a concentration at which the enzyme is mainly in a dimeric form, and also at 20 nM, showing at both concentrations very similar Hill coefficients (*40*), the result is that, at the lowest dilution, most of this enzyme exists as a dimer. More precisely, n is, on average, 1.4 for dimeric GST (*40*), while an n of 1 is expected for the monomeric enzyme. Via approximation of a linear dependence of the Hill coefficient on the degree of monomerization, the experimental error of $<8\%$ (*40*) implies a monomeric fraction of $<28\%$ at 20 nM, with a corresponding K_d of <4 nM, a value approximately 1000 times lower than the one calculated in previous studies (5.1 μM) (*22*).

Cooperativity for GSH Binding in GSTP1-1 Mutants Confirms Their Dimeric Structures at Nanomolar Levels. C47S and K54A are specific mutants of GSTP1-1 that in the past have been designed and expressed to verify the involvement of Cys 47 and Lys 54 in the stabilization of helix 2 (*42*, *43*). These specific mutants exhibited a positive cooperative binding of GSH, revealing for the first time the occurrence of intersubunit communication in GSTs. The Hill coefficients were 1.4−1.5 for both mutated enzymes. Even in that case, the homotropic behavior was evident at ~20−40 nM enzyme and also confirmed (with similar Hill coefficients) at much higher enzyme concentrations (*42*). In that previous study, no standard errors were reported for the Hill coefficients (*42*, *43*), but they are now recalculated from the original data, resulting in a value of $<10\%$. All differences between the observed n values fall well within this error interval. On the basis of the considerations discussed in the paragraph given above, these data indicate a monomerization level of $<35\%$ at 20 nM, with a resulting K_d of <7.5 nM.

Cooperative Self-Preservation Is Additional Evidence for a Dimeric Structure of GSTP1-1 at Nanomolar Levels. A few years ago, we observed that GSTP1-1 displays a peculiar mechanism that minimizes the deleterious effects of inactivating compounds once a first subunit of the dimer is modified (*44*). This process, triggered by alkylating compounds, thermal stress, UV irradiation, etc., has been explained assuming that the perturbation of one subunit causes a structural modification in the adjacent subunit that becomes more protected against further chemical or physical perturbations. This property, termed cooperative self-preservation, requires an oligomeric structure, and it has been observed at GST concentrations commonly used for assay measurements (20−40 nM). Thus, this finding provides now a further strong indication the enzyme must exist as a dimer at these low concentrations. For a quantitative evaluation of the maximal degree of monomerization consistent with these data, we consider that negative cooperativity parallels the behavior of two enzyme populations with different reactivities but with an equal population of the two forms. Therefore, the monomerization of a dimeric cooperative enzyme must be signaled by a significant increase of one population compared to the other. However, in our old data, the two populations ranged always from 45 to 55% (*44*), and therefore, the level of monomerization was $<10\%$. On this basis, the resulting K_d value is <0.5 nM.

Cooperative Binding of Dinitrosyl-Diglutathionyl-Iron Complex as a Probe for the Dimeric State of Alpha, Pi, and Mu GSTs. Alpha, pi, and mu class GSTs bind with extraordinary affinity the dinitrosyl-diglutathionyl-iron complex, a natural compound that is spontaneously produced when NO enters the cell (*45*, *46*). The calculated K_i values are approximately 10^{-9}−10^{-10} M. This strong interaction is possibly aimed at the storage of NO inside the cell and at the sequestration of the free form of DNDGIC that irreversibly inactivates key redox enzymes like glutathione reductase (*47*). Indeed, DNDGIC bound to GSTs becomes fully harmless for glutathione reductase (*8*). Binding of DNDGIC is characterized by negative cooperativity in all three isoezymes. For GSTP1-1 and GSTM2-2, this cooperativity is revealed by a peculiar inactivation behavior at different DNDGIC concentrations (that appears clearly biphasic). Binding of DNDGIC to GSTA1-1 is again cooperative, but it is accompanied by a particular effect, i.e., the total loss of activity when only one subunit of the dimer has bound one molecule of DNDGIC (*45*). Both cooperativity and overinhibition (for the alpha class GST) are likely due to intersubunit communication and would not be present if the enzymes were in a monomeric form. Given that negative cooperativity has been observed at 2−4 μM levels, but also down to 40 nM for GSTP1-1 and down to 20 nM for GSTM2-2, it results that the enzyme is mainly dimeric even at the lowest concentrations. Even in this case, inhibition data at the lowest concentration fit well to a system composed by a 50/50 mixture of two species with different affinities. More specifically, since the recovered value for the two populations is 50 ± 6%, we can assume that the level of monomerization is less than 12%, with a corresponding K_d value for the monomer-to-dimer transition of <1.3 nM for the pi class GSTs, and <0.6 nM for GSTM2-2. Also, the atypical overinhibition of GSTA1-1, equally indicative of intersubunit communication, has been found at 20 nM, thereby restricting its K_d value to <5 nM.

To better define the K_d range, we tried to verify if the cooperative behavior is still evident even at lower concentrations.

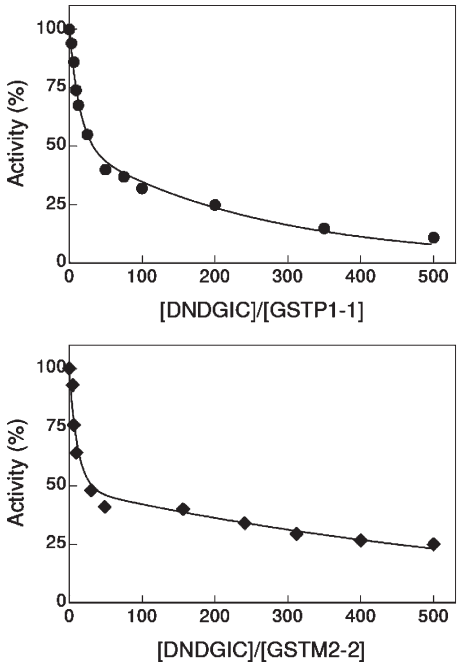

FIGURE 4: GSTP1-1 and GSTM2-2 negative cooperativity in DNDGIC binding at extreme dilutions. Human purified GSTP1-1 and GSTM2-2 were incubated for 1 min with variable amounts of DNDGIC at pH 7.4. Aliquots were then diluted in the assay mixture containing 1 mM GSH and 1 mM CDNB in the presence of 0.1 M potassium phosphate buffer (pH 6.5) at 25 °C. The final enzyme concentration in the assay mixture was 0.8 nM for GSTP1-1 (0.02 μg/mL) and 0.32 nM for GSTM2-2 (0.008 μg/mL). Solid lines are the best fits of the experimental points obtained for GSTP1-1 and GSTM2-2 to a biexponential decay equation. Experimental errors on data points do not exceed 7%.

Table 1: Effect of the Removal of Intersubunit Electrostatic Stabilization of GSH in the G-Site of GSTs

	K_m^{GSH}(Asp mutant)/ K_m^{GSH} (wild-type hGSTs) (experimental values for specific Asp mutants)	K_d^{D*}/K_d^{Da} (calculated for GST dimers after neutralization of selected Asp residues)
GSTP1-1	5.5[b]	3.1
GSTA1-1	5[c]	4.3
GSTM2-2	−	3.0

[a] K_d^{D*} values are the dissociation constants for the E−GSH complex calculated on the basis of docking of GSH to dimeric hGSTs after neutralization of the Asp residue (D*) participating in the stabilization of GSH in the adjacent subunit (Asp 98 for GSTP1-1, Asp 101 for GSTA1-1, and Asp 105 for GSTM2-2). [b] From ref *48*. [c] Obtained from values reported in ref *49*.

As shown in Figure 4, both GSTP1-1 and GSTM2-2 exhibit a strong negative cooperativity down to 0.02 μg/mL (0.8 nM) and at 0.008 μg/mL (0.3 nM), respectively, indicating that a dimeric structure is still predominant at such low levels. Again, these data fit well to a system composed of high- and low-affinity species with relative populations of 50 ± 7.5% for GSTP1-1 and 50 ± 10% for GSTM2-2. From these results, the corresponding K_d values for the monomer−dimer equilibrium must be confined to an even lower range, in particular, < 0.04 nM for GSTP1-1 and < 0.03 nM for GSTM2-2. Due to sensitivity problems, the overinhibition phenomenon caused by DNDGIC binding to GSTA1-1 could be observed only down to 4 nM enzyme (not shown), thus confining K_d values to < 1 nM.

Invariability of K_m^{GSH} Values as a Probe for a Dimeric State of Pi, Alpha, and Mu Class GSTs. GSH is stabilized in the G-site of GSTP1-1, GSTA1-1, and GSTM2-2 by a few electrostatic interactions with residues of the same subunit and by an additional interaction involving the carboxylate of the neighboring subunit. More precisely, the carboxylate group of Asp 98 of GSTP1-1 participates in the binding of GSH through electrostatic interaction with the amino group of the γ-glutamyl residue of GSH. Similarly, Asp 101 and Asp 105 fulfill additional electrostatic stabilizations of GSH in the G-sites of GSTA1-1 and GSTM2-2, respectively. GSH bound to GSTA1-1 also displays a further salt bridge between Arg 131 of the opposite subunit and the α-carboxyl group of the glutamyl residue of GSH. A direct confirmation of these intersubunit stabilizations came in the form of site-directed mutagenesis experiments performed by two different groups. Replacement of Asp 98 with Ala in GSTP1-1 increases 5.5-fold the K_m^{GSH} value (*48*), and a similar increase has been observed for GSTA1-1 when Asp 101 is replaced with Asn (*49*) (see Table 1). This lowered affinity toward GSH in these specific mutants of GSTP1-1 and GSTA1-1 represents now a further confirmation that both these isoenzymes must be dimers under standard assay test conditions (~20−40 nM). In fact, no difference in K_m^{GSH} values is expected as a consequence of these mutations if these enzymes exist as monomers under the standard assay conditions. Again, the estimated K_d values must be < 20 nM. To further confirm that intersubunit interactions contribute significantly to the substrate binding energy, we performed docking simulations on the native GST dimers and compared them with the same calculations executed after neutralization of Asp 98, Asp 101, or Asp 105 (in GSTP1-1, GSTA1-1, and GSTM2-2, respectively) in one subunit. These simulations predict a 3−4-fold loss of affinity as a consequence of Asp neutralization, a loss approaching the values observed experimentally in the D98A and D101N GST mutants (Table 1).

In this context, we tried to check experimentally possible changes in K_m^{GSH} values under extreme dilution conditions as a probe for the presence or absence of the monomerization process. As shown in Figure 5, we observed identical K_m^{GSH} values at 1 and 0.04 μg/mL for both GSTP1-1 and GSTA1-1 (~40 and 1.5 nM, respectively) and at 0.2 and 0.008 μg/mL for GSTM2-2 (~8 and 0.3 nM, respectively). These results indicate that the GST aggregation state is unchanged in this concentration range. The proof that under these highly dilute conditions all these enzyme are mainly in a dimeric form has been obtained by observing very similar K_d^{GSH} values measured via fluorescence experiments at 100 μg/mL (where GSTs are surely in a dimeric state) and K_d^{GSH} values calculated at very low enzyme concentrations by extrapolating K_m^{GSH} values at 0 mM CDNB. In fact, it is well-known that CDNB binding slightly alters the K_d^{GSH} (see Figure 5). The upper limits for K_d values can be determined by considering that the standard errors for the K_d^{GSH} values are always less than 20% for all isoenzymes. Since K_d^{GSH} for the monomer is 4−5 times higher than that of the dimeric enzyme (Table 1), a 20% variation in K_d^{GSH} would be caused by a 5−7% monomerization. Thus, K_d values are < 20 pM for alpha and pi GSTs and < 3 pM for mu class GSTs.

Equilibrium Problem. All the fluorescence and kinetic experiments described above provide a realistic estimation of K_d values only if these measurements have been performed under equilibrium conditions. More precisely, given that all these experiments started from concentrated enzyme stock solutions (where GSTs are likely under dimeric conditions) to reach the dilute levels used for fluorescence or kinetic experiments, it is necessary to prove that the monomerization process is fast enough to reach a final state of equilibrium within the period used for measurements. For this purpose, we measured the K_m^{GSH} values of GSTP1-1, GSTA1-1, and GSTM2-2 1 and 120 min after dilution in the assay test. Results reported in Table 2 indicate that no change occurred, suggesting that all kinetic and fluorescence measurements (made within 1−2 min of mixing the enzyme in the assay test) have been performed under equilibrium conditions or, alternatively, that the monomerization process occurs at very low rates ($t_{1/2}$ > 4 h). We also noted that at extreme dilution levels all these enzymes undergo a slow inactivation that ends at ~50% of the original activity. This inactivation has been observed previously for GSTP1-1 and explained on the basis of a solvation of the active site (*44*, *50*). Under our conditions [pH 6.5, 1 mM GSH, 4 nM GSTs (0.08 nM for GSTM2-2)], the apparent $t_{1/2}$ of the inactivation process that ends at 50% of the original activity is > 60 min for GSTA1-1 and GSTM2-2 and > 20 min for GSTP1-1 (not shown). As we will discuss below, these slow kinetics allow us to exclude the possibility that the observed inactivation is related to a synchronous monomerization process.

DISCUSSION

Steady-state and time-resolved fluorescence anisotropy, two-photon fluorescence correlation spectroscopy experiments, and new and old kinetic experiments have been used to re-examine the question of the monomer−dimer equilibrium of GSTs. The invariance of both cooperativity and affinity for GSH has also been employed like new probes to verify the persistence of a dimeric state at dilution levels below the detection limits of the fluorescence methodology. All data collected here definitively confine the K_d values in the nanomolar or subnanomolar field for three representative alpha, mu, and pi GST isoenzymes,

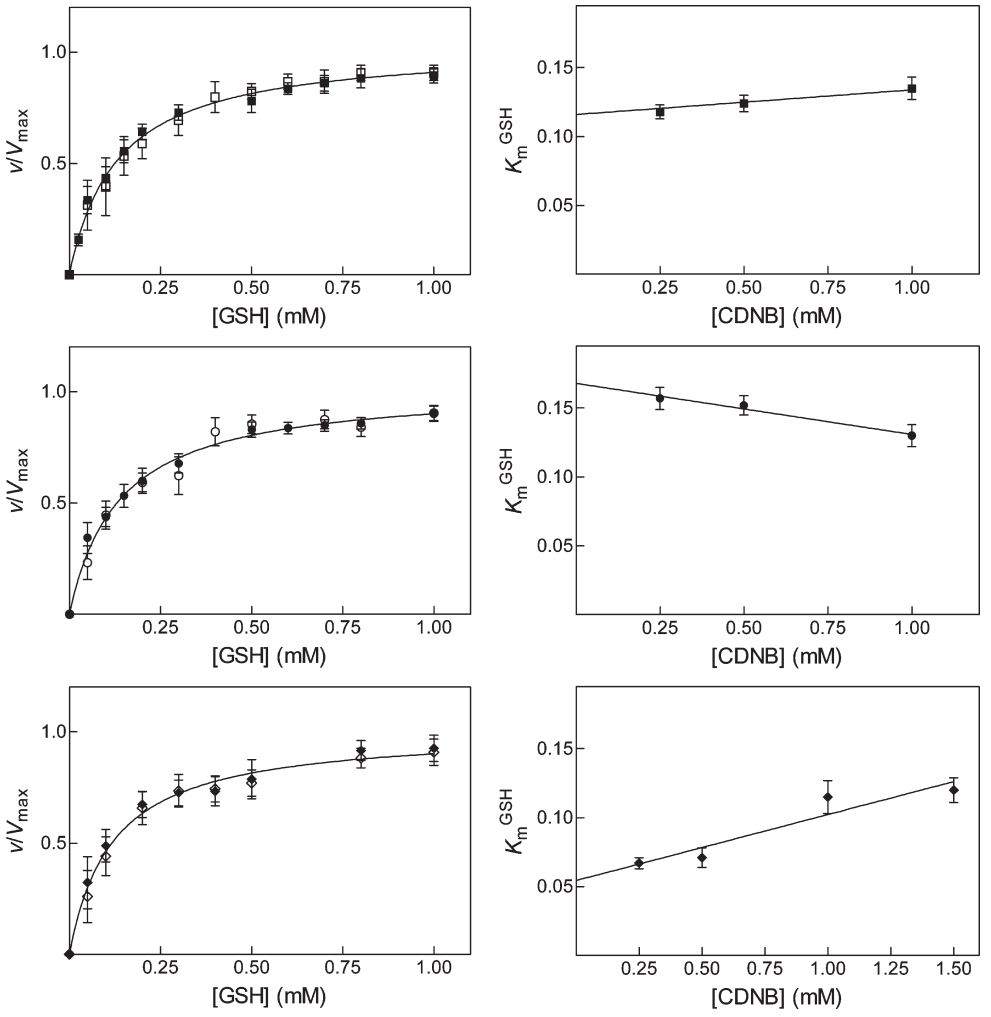

FIGURE 5: GSH binding at different hGSTs concentrations and relative dependence of K_m^{GSH} on CDNB concentration. Left panels show GSH binding at two different hGST concentrations for each isoform: GSTP1-1 at 1 (■) and 0.04 μg/mL (□), GSTA1-1 at 1 (●) and 0.04 μg/mL (○), and GSTM2-2 at 0.2 (◆) and 0.008 μg/mL (◇). Curves represent the best fits for each double-concentration data set. For experiments reported in the right panels, a fixed GSH concentration (1 mM) and CDNB concentrations varying from 0.25 mM to 1.5 mM have been used. Enzyme concentrations were: 1 μg/mL for GSTP1-1 (■), 1 μg/mL for GSTA1-1 (●), and 0.2 μg/mL for GSTM2-2 (◆). Solid lines show the dependence of K_m^{GSH} values on CDNB concentration. All values reported represent the means of at least three different experimental sets.

Table 2: K_d and K_m Values for GSH at Different hGSTs Concentrations

	K_m^{GSH} (mM) (at 1.0 and 0.04 μg/mL GST)	K_m^{GSH} (mM) (at 0.04 μg/mL GST after preincubation for 2 h)	K_d^{GSH} (mM) (from kinetic data)[a]	K_d^{GSH} (mM) (from fluorescence data at 100 μg/mL GST)	expected K_d^{GSH}(mM) for single monomers[b]
GSTP1-1	0.14 ± 0.01	0.15 ± 0.02	0.120 ± 0.003	0.13 ± 0.01	0.40
GSTA1-1	0.13 ± 0.01	0.16 ± 0.01	0.160 ± 0.004	0.16 ± 0.02	0.69
GSTM2-2	0.11 ± 0.01[c]	0.11 ± 0.03[d]	0.055 ± 0.001	0.050 ± 0.006	0.15

[a]Values obtained by extrapolating K_m^{GSH} data (obtained at different CDNB concentrations) to 0 mM CDNB (see Figure 5). [b]Calculated by multiplying K_d^{GSH} values (from fluorescence data) by the K_d^{D*}/K_d^{D} ratio listed in Table 1. [c]Concentrations of 0.2 and 0.008 μg/mL for GSTM2-2. [d]Concentration of 0.008 μg/mL for GSTM2-2.

i.e., GSTA1-1, GSTM2-2, and GSTP1-1 (see Scheme 1). The possibility that kinetic or fluorescence measurements were performed under nonequilibrium conditions and that monomerization was not attained on the time scale of our experiments should be discussed. The invariance of K_m observed after incubation for 1 and 120 min under dilute enzyme conditions (see Table 2) is diagnostic in this context. Assuming that GST monomerization would have been attained on a longer time scale, the $t_{1/2}$ for the monomerization event must be longer than at least 2 times the t_{obs}; i.e., $t_{1/2} > 4$ h. Experimental observation on longer time scales is prevented by denaturation problems. In any case, these data set an upper limit on their k_{off} values for the equilibrium $M+M \underset{k_{off}}{\overset{k_{on}}{\rightleftarrows}} D$ that must be $< 5 \times 10^{-5}$ s^{-1}. The k_{on} value for the monomer−monomer association of GSTs is not known, but for many proteins, it is diffusion-limited and ranges from 10^6 M^{-1} s^{-1} (for monomers that are not linked by electrostatic forces) to 10^9 M^{-1} s^{-1} (for monomers that display electrostatic interactions at the dimer interface) (*51*−*54*). Alpha, pi, and mu GSTs have a number of electrostatic interactions at the dimer interface, but even considering a k_{on} of only 10^6 M^{-1} s^{-1}, the resulting $K_d = k_{off}/k_{on}$ must be $< 5 \times 10^{-11}$ M. Thus, even assuming a nonequilibrium condition in many of our

Scheme 1: Cumulative Scheme of K_d Values Coming from This Study and Previous Studies[a]

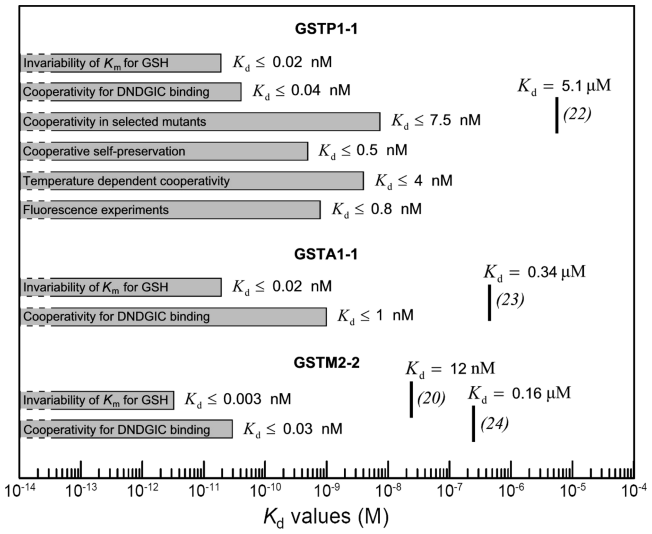

[a]Horizontal bars represent the range of possible K_d values estimated in this study. Vertical bars indicate the K_d values reported in previous studies (references are also shown).

experimental approaches, the overall K_d value for the monomer-to-dimer transition must be confined invariably at or below the nanomolar range. A similar conclusion can be drawn by assuming that the slow inactivation process observed at high dilution is related to a monomerization event that causes a complete inactivation of the enzyme. In this case, no change in K_m is expected but only a loss of V_{max}. However, the very slow inactivation process [$k_{inact} \leq 0.001$ s^{-1} for GSTP1-1 (*44*), and $k_{inact} \leq 10^{-4}$ s^{-1} for GSTM2-2 and GSTA1-1], if synchronous to the monomerization process ($k_{inact} = k_{off}$), restricts invariably the K_d values in the subnanomolar range ($k_{off}/k_{on} < 10^{-3}$ $s^{-1}/10^6$ M^{-1} $s^{-1} < 10^{-9}$ M^{-1}). Finally, the possibility that the inactivation is slower than the monomerization is unlikely. In fact, the presence of an active monomer can be excluded on the basis of the invariance of K_d values (see Table 2).

At this point, it is difficult to explain the high K_d values found in previous investigations (*22*−*24*). These studies are based mainly on light scattering measurements and sedimentation equilibrium experiments. Although all these experiments appear to be well performed and statistically validated, we underline that the range of applicability of the light scattering approach is limited by the protein concentration and by the molecular mass of the protein studied. For example, for the Wyatt miniDAWN light scattering instrument (used for most of the previous studies), the suggested concentration range for macromolecules of molecular mass of 200 kDa is from 2 to 0.2 mg/mL (miniDAWN user's booklet). For a molecular mass of 45−50 kDa, as in the case of GSTs, the concentration range would be limited to even higher concentrations. It is then possible that measurements using very low protein concentrations (down to 0.03 mg/mL), as performed in the previous studies cited above, could have generated artifactual low mass estimations that could have been interpreted as a signal of an incipient monomerization. Similarly, sedimentation equilibrium experiments with native GSTs under mild conditions only showed very small changes in the average molecular mass that could be again interpreted as a partial monomerization, while they could be due only to instrumental limits.

The shift of K_d values from the micromolar level to the nanomolar or subnanomolar level for the monomer−dimer equilibrium of alpha, pi, and mu GSTs severely impairs the hypothesis for the existence of fully active GST monomers. Indeed, on the basis of the K_d values previously calculated from sedimentation experiments and light scattering measurements [5.1 μM for GSTP1-1 (*22*), 0.34 μM for GSTA1-1 (*23*), and 0.45 μM for GSTM2-2 (*24*)], Colman and coworkers concluded that these enzymes exist mainly in a monomeric state when they are assayed under the usual activity test conditions (0.2−1 μg/mL). Thus, pi and mu isoenzymes in the monomeric form would be active, and paradoxically, all previous reported specific activities cannot be referred to the dimeric structure of GSTs but to their corresponding monomers. Obviously, these conclusions cannot be drawn on the basis of the new K_d values that are < 1 nM. These new values indicate the prevalence of the dimeric form even at very low enzyme concentrations. The consequence is that at present it is not possible to ascertain if the monomer is fully active or inactive, simply because the monomer cannot be observed even at very low enzyme concentrations.

For the sake of completeness, we would like to mention that the mutated GSTP1-1 designed by Abdalla et al. (*17*) is fully monomeric and appears structurally stable but completely inactive, and similar evidence has been reported by Aceto et al. (*16*) after monomerization of GSTP1-1 with mild detergents. The same inactivation has been reported for a few mutants of GSTM2-2, in particular, for the F56S/R81A double mutant that appears mainly monomeric but has a severely impaired catalytic activity (*21*). Finally, it has been reported that among many GSTA1-1 mutants, only the mutant enzyme R69E exists mainly as a monomer and displays some activity (~15% of that of the dimer) (*23*), while the F52A mutant, which also is mainly monomeric, has lost its catalytic activity (*23*). Even in this case, however, calculation of monomer and dimer levels has been conducted using light scattering approaches. Thus, although no unequivocal proof of an active or inactive GSTs monomer is now available, many reports suggest that an isolated subunit could be fully inactive or very scarcely active.

From a physiological point of view, the data presented here are particularly relevant. A few studies reported the identification of monomeric GST inside the cells using antibody reactions or MALDI-TOF analysis (*4*, *18*). However, the confinement of K_d values for the monomer−dimer equilibrium to the nanomolar range indicates that very small amounts of GST monomers must be found inside the cells unless post-translational modifications or denaturation events reduced the affinity of each monomer for the adjacent subunit. The recent observation of the monomeric form of GSTP1-1 in human erythrocytes, exhibiting a peculiar phosphorylated serine (Ser 196) (*18*), seems to confirm this hypothesis.

REFERENCES

1. Mannervik, B., and Danielson, U. H. (1988) Glutathione transferases: Structure and catalytic activity. *CRC Crit. Rev. Biochem. 23*, 283–337.
2. Hayes, J. D., and Pulford, D. J. (1995) The glutathione S-transferase supergene family: Regulation of GST and the contribution of the isoenzymes to cancer chemoprotection and drug resistance. *CRC Crit. Rev. Biochem. Mol. Biol. 30*, 445–600.
3. Boyer, T. D., Vessey, D. A., Holcomb, C., and Saley, N. (1984) Studies of the relationship between the catalytic activity and binding of non-substrate ligands by the glutathione S-transferases. *Biochem. J. 217*, 179–185.
4. Adler, V., Yin, Z., Fuchs, S. Y., Benezra, M., Rosario, L., Tew, K. D., Pincus, M. R., Sardana, M., Henderson, C. J., Wolf, C. R., Davis, R. J., and Ronai, Z. (1999) Regulation of JNK signaling by GSTp. *EMBO J. 18*, 1321–1334.

5. Cho, S.-G., Lee, Y. H., Park, H.-S., Ryoo, K., Kang, K. W., Park, J., Eom, S.-J., Kim, M. J., Chang, T. S., Choi, S.-Y., Shim, J., Kim, Y., Dong, M.-S., Lee, M.-J., Kim, S. G., Ichijo, H., and Choi, E.-J. (2001) Glutathione S-transferase mu modulates the stress-activated signals by suppressing apoptosis signal-regulating kinase 1. *J. Biol. Chem. 276*, 12749–12755.
6. Gilot, D., Loyer, P., Corlu, A., Glaise, D., Lagadic-Gossmann, D., Atfi, A., Morel, F., Ichijo, H., and Guguen-Guillouzo, C. (2002) Liver protection from apoptosis requires both blockage of initiator caspase activities and inhibition of ASK1/JNK pathway via glutathione S-transferase regulation. *J. Biol. Chem. 277*, 49220–49229.
7. Bernardini, S., Bernassola, F., Cortese, C., Ballerini, S., Melino, G., Motti, C., Bellincampi, L., Iori, R., and Federici, G. (2000) Modulation of GST P1-1 activity by polymerization during apoptosis. *J. Cell. Biochem. 77*, 645–653.
8. Pedersen, J. Z., De Maria, F., Turella, P., Federici, G., Mattei, M., Fabrini, R., Dawood, K. F., Massimi, M., Caccuri, A. M., and Ricci, G. (2007) Glutathione Transferases Sequester Toxic Dinitrosyl-Iron Complexes in Cells. *J. Biol. Chem. 282*, 6364–6371.
9. Mannervik, B., Ålin, P., Guthenberg, C., Jensson, H., Tahir, M. K., Warholm, M., and Jornvall, H. (1985) Identification of three classes of cytosolic glutathione transferase common to several mammalian species: Correlation between structural data and enzymatic properties. *Proc. Natl. Acad. Sci. U.S.A. 82*, 7202–7206.
10. Meyer, D. J., Coles, B., Pemble, S. E., Gilmore, K. S., Fraser, G. M., and Ketterer, B. (1991) Theta, a new class of glutathione transferases purified from rat and man. *Biochem. J. 274*, 409–414.
11. Buetler, T. M., and Eaton, D. L. (1992) Glutathione S-transferases: Amino acid sequence comparison, classification and phylogenetic relationship. *J. Environ. Sci. Health, Part C: Environ. Carcinog. Ecotoxicol. Rev. 10*, 181–203.
12. Pemble, S. E., Wardle, A. F., and Taylor, J. B. (1996) Glutathione S-transferase class kappa: Characterization by the cloning of rat mitochondrial GST and identification of a human homologue. *Biochem. J. 319*, 749–754.
13. Board, P. G., Baker, R. T., Chelvanayagam, G., and Jermiin, L. S. (1997) Zeta, a novel class of glutathione transferases in a range of species from plants to humans. *Biochem. J. 328*, 929–935.
14. Board, P. G., Coggan, M., Chelvanayagam, G., Easteal, S., Jermiin, L. S., Schulte, G. K., Danley, D. E., Hoth, L. R., Griffor, M. C., Kamath, A. V., Rosner, M. H., Chrunyk, B. A., Perregaux, D. E., Gabel, C. A., Geoghegan, K. F., and Pandit, J. (2000) Identification, Characterization, and Crystal Structure of the Omega Class Glutathione Transferases. *J. Biol. Chem. 275*, 24798–24806.
15. Mannervik, B., Board, P. G., Hayes, J. D., Listowsky, I., and Pearson, W. R. (2005) Nomenclature for mammalian soluble glutathione transferases. *Methods Enzymol. 401*, 1–8.
16. Aceto, A., Caccuri, A. M., Sacchetta, P., Bucciarelli, T., Dragani, B., Rosato, N., Federici, G., and Di Ilio, C. (1992) Dissociation and unfolding of Pi-class glutathione transferase. *Biochem. J. 285*, 241–245.
17. Abdalla, A.-M., Bruns, C. M., Tainer, J. A., Mannervik, B., and Stenberg, G. (2002) Design of a monomeric human glutathione transferase GSTP1, a structurally stable but catalytically inactive protein. *Protein Eng. 15*, 827–834.
18. T. Kura, T., Takahashi, Y., Takayama, T., Ban, N., Saito, T., Kuga, T., and Niitsu, Y. (1996) Glutathione s-transferase-p is secreted as a monomer into human plasma by platelets and tumor cells. *Biochim. Biophys. Acta 1292*, 317–323.
19. Sayed, Y., Wallace, L. A., and Dirr, H. W. (2000) The hydrophobic lock-and-key intersubunit motif of glutathione transferase A1-1: Implications for catalysis, ligandin function and stability. *FEBS Lett. 465*, 169–172.
20. Hornby, J. A. T., Codreanu, S. G., Armstrong, R. N., and Dirr, H. W. (2002) Molecular recognition at the dimer interface of a class Mu glutathione transferase: Role of a hydrophobic interaction motif in dimer stability and protein function. *Biochemistry 41*, 14238–14247.
21. Thompson, L. C., Walters, J., Burke, J., Parson, J. F., Armsrong, R. N., and Dirr, H. W. (2006) Double mutation at the subunit interface of glutathione transferase rGSTM1-1 results in a stable, folded monomer. *Biochemistry 45*, 2267–2273.
22. Huang, Y. C., Misquitta, S., Blond, S. Y., Adams, E., and Colman, R. F. (2008) Catalytically Active Monomer of Glutathione S-Transferase π and Key Residues Involved in the Electrostatic Interaction between Subunits. *J. Biol. Chem. 283*, 32880–32888.
23. Vargo, M. A., Nguyen, L., and Colman, R. F. (2004) Subunit interface residues of glutathione S-transferase A1-1 important in the monomer/dimer equilibrium. *Biochemistry 43*, 3327–3335.
24. Hearne, J. L., and Colman, R. F. (2006) Catalytically active monomer of class Mu glutathione transferase from rat. *Biochemistry 45*, 5974–5984.
25. Lo Bello, M., Nuccetelli, M., Caccuri, A. M., Stella, L., Parker, M. W., Rossjohn, J., McKinstry, W. J., Mozzi, A. F., Federici, G., Polizio, F., Pedersen, J. Z., and Ricci, G. (2001) Human Glutathione Transferase P1-1 and Nitric Oxide Carriers. *J. Biol. Chem. 276*, 42138–42145.
26. Board, P. G., and Pierce, K. (1987) Expression of human glutathione S-transferase 2 in *Escherichia coli*. Immunological comparison with the basic glutathione S-transferases isoenzymes from human liver. *Biochem. J. 248*, 937–941.
27. Ross, V. L., and Board, P. G. (1993) Molecular cloning and heterologous expression of an alternatively spliced human Mu class glutathione S-transferase transcript. *Biochem. J. 294*, 373–380.
28. Gill, S. G., and Von Hippel, P. H. (1989) Calculation of protein extinction coefficients from amino acid sequence data. *Anal. Biochem. 182*, 319–326.
29. Ellman, G. L. (1959) Tissue sulfhydryl groups. *Arch. Biochem. Biophys. 82*, 70–77.
30. Morris, G. M., Goodsell, D. S., Halliday, R. S., Huey, R., Hart, W. E., Belew, R. K., and Olson, A. J. (1998) Automated Docking Using a Lamarckian Genetic Algorithm and and Empirical Binding Free Energy Function. *J. Comput. Chem. 19*, 1639–1662.
31. Weiner, S. J., Kollman, P. A., Case, D. A., Singh, U. C., Ghio, C., Alagona, G., Profeta, S., and Weiner, P. (1984) A new force field for molecular mechanical simulation of nucleic acids and proteins. *J. Am. Chem. Soc. 106*, 765–784.
32. Gasteiger, J., and Marsili, M. (1980) Iterative Partial Equalization of Orbital Electronegativity: A Rapid Access to Atomic Charges. *Tetrahedron 36*, 3219–3228.
33. Koradi, R., Billeter, M., and Wüthrich, K. (1996) MOLMOL: A program for display and analysis of macromolecular structures. *J. Mol. Graphics 14*, 51–55.
34. Lakowicz, J. R. (2006) Principles of Fluorescence Spectroscopy , pp 353−412, Springer, New York.
35. Liebau, E., Dawood, K. F., Fabrini, R., Fisher-Riepe, L., Perbandt, M., Stella, L., Pedersen, J. Z., Bocedi, A., Petrarca, P., Federici, G., and Ricci, G. (2009) Tetramerization and Cooperativity in *Plasmodium falciparum* Glutathione S-Transferase Are Mediated by Atypic Loop 113−119. *J. Biol. Chem. 284*, 22133–22139.
36. Folcarelli, S., Battistoni, A., Carrì, M. T., Polticelli, F., Falconi, M., Nicolini, L., Stella, L., Rosato, N., Rotilio, G., and Desideri, A. (1996) Effect of Lys-Arg mutation on the thermal stability of Cu,Zn superoxide dismutase: Influence on the monomer-dimer equilibrium. *Protein Eng. 9*, 323–325.
37. Yguerabide, J. (1972) Nanosecond fluorescence spectroscopy of macromolecules. *Methods Enzymol. 26*, 498–578.
38. Lakowicz, J. R. (2006) Principles of Fluorescence Spectroscopy, pp 798−840, Springer, New York.
39. Young, M. E., Carroad, P. A., and Bell, R. L. (1980) Estimation of Diffusion Coefficients of Proteins. *Biotechnol. Bioeng. 22*, 947–955.
40. Caccuri, A. M., Antonini, G., Ascenzi, P., Nicotra, M., Nuccetelli, M., Mazzetti, A. P., Federici, G., Lo Bello, M., and Ricci, G. (1999) Temperature Adaptation of Glutathione S-Transferase P1-1. *J. Biol. Chem. 274*, 19276–19280.
41. Hitchens, T. K., Mannervik, B., and Rule, G. S. (2001) Disorder-to-order transition of the active site of human class Pi glutathione transferase, GST P1-1. *Biochemistry 40*, 11660–11669.
42. Ricci, G., Lo Bello, M., Caccuri, A. M., Pastore, A., Nuccetelli, M., Parker, M. W., and Federici, G. (1995) Site-directed Mutagenesis of Human Glutathione Transferase P1-1. *J. Biol. Chem. 270*, 1243–1248.
43. Lo Bello, M., Battistoni, A., Mazzetti, P., Board, P. G., Muramatsu, M., Federici, G., and Ricci, G. (1995) Site-directed Mutagenesis of Human Glutathione Transferase P1-1. *J. Biol. Chem. 270*, 1249–1253.
44. Ricci, G., Caccuri, A. M., Lo Bello, M., Parker, M. W., Nuccetelli, M., Turella, P., Stella, L., Di Iorio, E., and Federici, G. (2003) Glutathione transferase P1-1: Self-preservation of an anti-cancer enzyme. *Biochem. J. 376*, 71–76.
45. De Maria, F., Pedersen, J. Z., Caccuri, A. M., Antonini, G., Turella, P., Stella, L., Lo Bello, M., Federici, G., and Ricci, G. (2003) The Specific Interaction of Dinitrosyl-Diglutathionyl-Iron Complex, a Natural NO Carrier, with the Glutathione Transferase Superfamily. *J. Biol. Chem. 278*, 42283–42293.
46. Turella, P., Pedersen, J. Z., Caccuri, A. M., De Maria, F., Mastroberardino, P., Lo Bello, M., Federici, G., and Ricci, G. (2003) Glutathione Transferase Superfamily Behaves Like Storage Proteins for Dinitrosyl-Diglutathionyl-Iron Complex in Heterogeneous Systems. *J. Biol. Chem. 278*, 42294–42299.

47. Keese, M. A., Böse, M., Mülsch, A., Schirmer, R. H., and Becker, K. (1997) Dinitrosyl-Dithiol-Iron Complexes, Nitric Oxide (NO) Carriers In Vivo, as Potent Inhibitors of Human Glutathione Reductase and Glutathione-S-Transferase. *Biochem. Pharmacol. 54*, 1307–1313.
48. Kong, K.-H., Inoue, H., and Takahashi, K. (1993) Site-directed Mutagenesis Study on the Roles of Evolutionally Conserved Aspartic Acid Residues in Human Glutathione S-Transferase P1-1. *Protein Eng. 6*, 93–99.
49. Wang, R. W., Newton, D. J., Huskey, S.-E. W., McKeever, B. M., Pickett, C. B., and Lu, A. Y. H. (1992) Site-directed Mutagenesis of Glutathione S-Transferase YaYa. *J. Biol. Chem. 267*, 19866–19871.
50. Adams, P. A., and Sikakana, C. N. T. (1990) Factors Affecting the inactivation of human placental glutathione S-transferase π. *Biochem. Pharmacol. 39*, 1883–1889.
51. Stone, R. S., Dennis, S., and Hofsteenge, J. (1989) Quantitative evaluation of the contribution of ionic interactions to the formation of the thrombin-hirudin complex. *Biochemistry 28*, 6857–6863.
52. Schreiber, G., and Fersht, A. R. (1996) Rapid, electrostatically assisted association of proteins. *Nat. Struct. Biol. 3*, 427–431.
53. Northrup, S. H., and Erickson, H. P. (1992) Kinetics of protein-protein association explained by Brownian dynamics computer simulation. *Proc. Natl. Acad. Sci. U.S.A. 89*, 3338–3342.
54. Schreiber, G., Haran, G., and Zhou, H.-X. (2009) Fundamental aspects of protein-protein association kinetics. *Chem. Rev. 109*, 839–860.